# Ion implantation investigation for the passivation of cut edge solar cells

Cyril Leon, Damien Barakel, Vitalie Burlac, Laurent Roux, Riadh Ben Abbes, Thomas Regrettier, Olivier Palais, Frank Torregrosa

# Ion Implantation Investigation for the Passivation of Cut Edge Solar Cells

Cyril Leon[1,a)] and Damien Barakel[1] and Vitalie Burlac[2] and Laurent Roux[3] and Riadh Ben Abbes[3] and Thomas Regrettier[2] and Olivier Palais[1,b)] and Frank Torregrossa[3].

Author Affiliations
[1] *IM2NP, UMR CNRS 6242, Aix-Marseille University, FST St Jérôme, Marseille Cedex 20, France.*
[2] *Voltec Solar, Dinsheim-sur-Bruche, France.*
[3] *Ion Beam Services (IBS), Rue Gaston Imbert Prolongée, ZI Rousset-Peynier, 13790 Peynier, France.*

*Author Emails*
[a)] Corresponding author: cyril.leon@im2np.fr
[b)] olivier.palais@univ-amu.fr

**Abstract.** This work aims to study the efficiency of ion implantation using P-III (Plasma-Immersion Ion Implantation) to passivate the cut edges of half Silicon HeteroJuntion (SHJ) and Tunnel Oxide Passivated Contact (TOPCon) technologies. The samples are cut using the Thermal Laser Separation process (TLS-Dicing$^{TM}$). Edge qualities and sample performances are measured via Light Beam Induced Current (LBIC) and Suns-Voc to evaluate the degradation after the cutting process. The Passivation by P-III is carried out under different conditions, varying the type of gas, the dose, the plasma mode and the plasma potential. Results show no significant gain when SHJ and TOPCon half cells are implanted using $H_2$ plasma gaz. However, the use of $O_2$ plasma to passivate TOPCon cut edges shows interesting results but need to be confirmed on a larger group of samples.

## INTRODUCTION

Silicon based solar cells have reached impressive conversion efficiencies, gradually approaching the Shockley-Queisser limit with a record at 26.7% for an IBC (Interdigitated Back Contact) solar cell developed in 2017 by K. Yoshikawa et al [1,2]. In parallel, the best module efficiency obtained with the same type of solar cell only reaches 24.4% [1,2]. Many studies have been published in order to understand and limit the losses when assembling the cells into modules. Among other issues, those researches highlight the important role of the resistive losses in the cells interconnections [3-10].

The use of cut cells has emerged as a possible alternative in order to limit these resistive losses. Indeed, with smaller cells connected in series, the current generated is lower and so are the resistive losses. However, the fabrication of cut cells brings new challenges such as the development of a low loss cutting technique or the passivation of the cut edge. Despite those challenges, this topic is important enough to find itself as one of the main objectives of a European project such as the H2020 HighLite project [11].

Regarding the cutting process challenges, different approaches have been studied in the literature: Mechanical Cleaving (MC) [12-15], Laser Scribbing and Mechanical Cleaving (LSMC) [16-22] and Thermal Laser Separation (TLS) [12,14,18,21-23]. Results show lower losses, higher mechanical strength and smoother edges when the latter technique is used. Regarding the passivation of the cut edge, some researches have investigated the use of different

coating materials such as SiNx [16], AlOx [23,24] or a-Si:H [15,25], giving mitigated results. In the best case, the coating and annealing process allowed to recover half of the losses due to the cutting process but in most studies, the passivation gave no significant improvement of the cut cell performances.

In our research, we propose to study a new approach to passivate the cut edge using Plasma-Immersion Ion Implantation (P-III). This method has the advantage of (i) already being used in the fabrication of some solar cells for the doping and the passivation of layers [26] and (ii) unlike coating, not being very sensitive to the roughness quality of the edge.

## MATERIAL AND METHOD

The interest of passivation using P-III is investigated on two efficient technologies: SHJ (Silicon HeteroJunction) and TOPCon (Tunnel Oxide Passivated Contact) solar cells whose best efficiency for large cells have reached respectively 25.8% and 25.2% [1,27]. The cells are cut using the TLS-Dicing™ technique to ensure the best edge quality. The degradation of the edge after the cut is observed using Light Beam Induced Current (LBIC) and quantified by Suns-$V_{OC}$ measurements. They are then passivated in a plasma chamber using the ©PULSION implanter (represented in Fig. 1). The cells are placed in the plasma chamber in such manner that the surfaces are protected and that the cut edge is the most exposed to the ions.

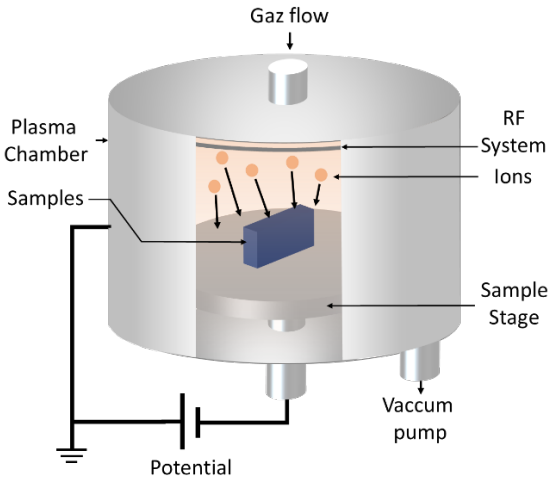


**FIGURE 1.** Schematic representation of the ©PULSION implanter.

Results of three campaigns of implantation are discussed in this article. Campaign n°1 aims to observe the impact of $H_2$ implantation and annealing on SHJ cut cells compared to full SHJ cells. Implantation and annealing parameters for this campaign are written in Table 1. Campaign n°2 seeks to compare different $H_2$ implantation conditions performed on SHJ half cells (parameters can be found in Table 2). Campaign n°3 explores this time the implantation of $H_2$ and $O_2$ on TOPCon cut cells using different plasma mode. The implantation and annealing parameters for this campaign are summarized in Table 3. In each campaign, several cells were kept un-implanted as references.

## RESULTS AND DISCUSSIONS

### Quality of the edges after the cut.

First, LBIC measurements were carried out on un-implanted samples. Figure 2 compares LBIC profiles probing the cut edges (red curves) with LBIC profiles probing the uncut edges (black curves) for the two types of technologies. TOPCon's profiles (Fig. 2a) clearly show a more gradual decrease of the LBIC signal near the cut edge which attests of its lower quality. SHJ's profiles (Fig. 2b) are more difficult to analyze since the uncut edge appears to be wider than the cut edge. This could be explained knowing that the TCO layer (Transparent Conductive Oxyde) is wider than the absorber in the SHJ cells causing reflections and a larger apparent edge. Because of this reflection artefact and of the metallization shading, it is difficult to quantify the degradation of the cut edges. However, one can still observe a

slightly decreased signal very near the cut edge. In the following sections, to properly quantify the degradation of the cells after the cutting process and any possible gain after the implantation and annealing processes, Suns-$V_{OC}$ measurements have been performed on different group of samples.

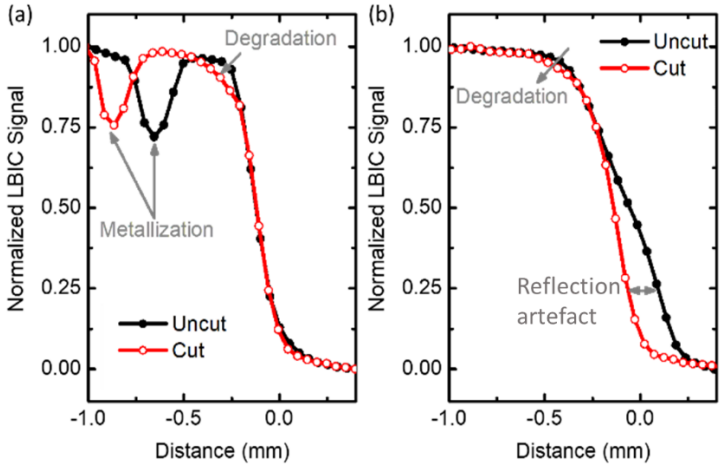


**FIGURE 2.** Normalized LBIC profils perpendicular to a cut edge compared to the one perpendicular to an uncut edge of an un-implanted (a) half TOPCon sample and (b) half SHJ sample.

## Campaign n°1: Impact of the cut, implantation and annealing on SHJ solar cells.

**TABLE 1.** Implantation and annealing parameters used for the campaign n°1.

| Technology | Format | P-III gas | P-III potential | P-III dose | Plasma mode | Annealing Temperature | Annealing time | Number of samples |
|---|---|---|---|---|---|---|---|---|
| SHJ | Full | - | - | - | - | 170°C | 10 min | 2 |
| | Full | H2 | 200 V | $10^{15}$ $cm^{-2}$ | Continuous | - | - | 3 |
| | Half | H2 | 200 V | $10^{15}$ $cm^{-2}$ | Continuous | 170°C | 10 min | 12 |

In this campaign, the pseudo-performances of 5 full SHJ solar cells are measured before any treatment to assess their initial quality. The same measurements are performed on a dozen of half SHJ cells and results are plotted in Fig. 3. A clear loss of approximately 0.2% of the pseudo-efficiency can be observed by comparing the performances of the full and half cells. Then, the half cells are implanted at low potential and medium dose using a continuous $H_2$ plasma. Pseudo-efficiencies of the half cells measured right after the implantation show a slight decrease. We have also performed the same implantation process but on 3 full SHJ solar cells showing the same order of magnitude of degradation, proving that due to $H_2$ implantation, not only the cut edges can be damaged but also the uncut edges. After the implantation, a 10 minutes annealing at 170°C is performed on the cut and implanted half SHJ cells and on two full SHJ un-implanted cells. In both cases we observe a small increase in the measured pseudo-efficiency. The fact that the same improvement in the performances can be observed on the full and un-implanted SHJ cells shows that the increase of the pseudo-efficiency might not be related neither to the cut nor to the implantation but that probably other areas of the samples are improved. We have also performed other series of annealing, but due to the maximum temperature that can accept the amorphous layer in the SHJ structure, higher temperature annealed cells only show a degradation of their performances again.

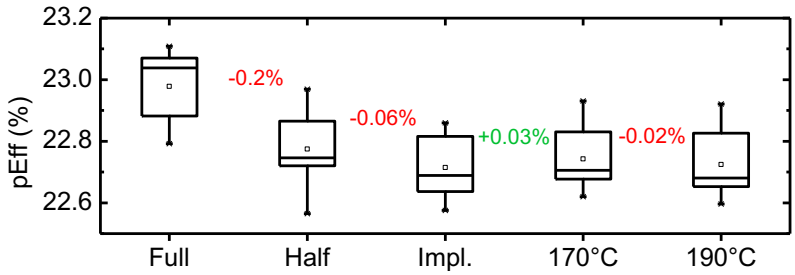


**FIGURE 3.** Pseudo-efficiencies measured on five full SHJ cells compared with the pseudo-efficiency measured on a dozen of half SHJ cells after the cut, after the $H_2$ implantation and after series of annealing at 170°C for 10 minutes then 190°C for 10 minutes.

## Campaign n°2: Investigating several $H_2$ implantation conditions on SHJ half cells.

**TABLE 2.** Implantation and annealing parameters used for the campaign n°2.

| Technology | Format | P-III gas | P-III potential | P-III dose | Plasma mode | Annealing Temperature | Annealing time | Number of samples |
|---|---|---|---|---|---|---|---|---|
| SHJ | Half | - | - | - | - | 170°C | 10 min | 12 |
| SHJ | Half | $H_2$ | 200 V | $5\times10^{14}$ cm$^{-2}$ | Continuous | 170°C | 10 min | 12 |
| SHJ | Half | $H_2$ | 200 V | $1\times10^{16}$ cm$^{-2}$ | Continuous | 170°C | 10 min | 12 |
| SHJ | Half | $H_2$ | 2500 V | $5\times10^{15}$ cm$^{-2}$ | Continuous | 170°C | 10 min | 12 |
| SHJ | Half | $H_2$ | 4800 V | $5\times10^{14}$ cm$^{-2}$ | Continuous | 170°C | 10 min | 11 |
| SHJ | Half | $H_2$ | 4800 V | $1\times10^{16}$ cm$^{-2}$ | Continuous | 170°C | 10 min | 9 |

In this part, more $H_2$ implantation conditions have been investigated on a large group of samples after the cutting process. Several half SHJ have been kept un-implanted as references to quantify the gain introduced by annealing without prior implantation. Then, varying the dose and the potential of the continuous $H_2$ plasma, five implantation conditions have been performed on the half SHJ cells. Results are shown in Fig. 4. For most of the investigated conditions, the same amount of degradation in the pseudo-efficiency is observed right after the implantation. After annealing, it appears that the performances that was lost du to the implantation have been recovered so that in the end, the implanted and annealed cells show the same performances than the un-implanted but annealed cells. Except for the condition with the highest potential and the highest dose implanted, where the damage after the implantation was to important.

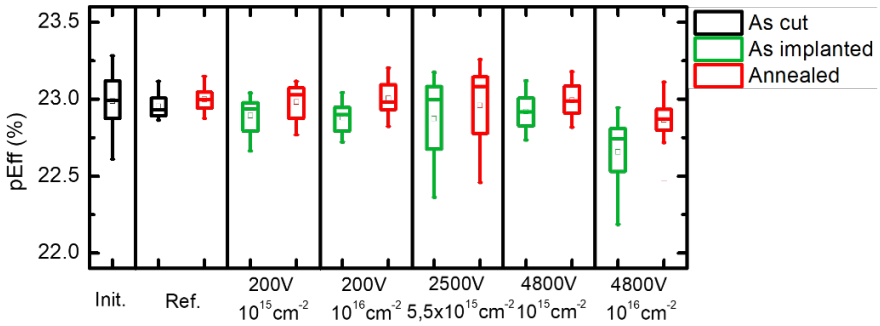


**FIGURE 4.** Pseudo-efficiency measured on a large group of SHJ half cells before any treatment, before and after annealing without prior passivation and before and after annealing with prior implantation.

## Campaign n°3: Investigating several $H_2$ and $O_2$ implantation conditions on TOPCon half cells.

**TABLE 3.** Implantation and annealing parameters used for the campaign n°3.

| Technology | Format | P-III gas | P-III potential | P-III dose | Plasma mode | Annealing Temperature | Annealing time | Number of samples |
|---|---|---|---|---|---|---|---|---|
| TOPCon | Half | - | - | - | - | 350°C | 10 min | 14 |
| TOPCon | Half | $O_2$ | 0 V | $1\times10^{16}$ cm$^{-2}$ | Pulsed | 350°C | 10 min | 2 |
| TOPCon | Half | $O_2$ | 100 V | $1\times10^{17}$ cm$^{-2}$ | Pulsed | 350°C | 10 min | 2 |
| TOPCon | Half | $O_2$ | 100 V | $5\times10^{15}$ cm$^{-2}$ | Pulsed | 350°C | 10 min | 2 |
| TOPCon | Half | $O_2$ | 5500 V | $5.5\times10^{15}$ cm$^{-2}$ | Pulsed | 350°C | 10 min | 2 |
| TOPCon | Half | $O_2$ | 1000 V | $1\times10^{16}$ cm$^{-2}$ | Pulsed | 350°C | 10 min | 2 |
| TOPCon | Half | $O_2$ | 1000 V | $1\times10^{17}$ cm$^{-2}$ | Pulsed | 350°C | 10 min | 2 |
| TOPCon | Half | $H_2$ | 200 V | $5\times10^{14}$ cm$^{-2}$ | Pulsed | 350°C | 10 min | 1 |
| TOPCon | Half | $H_2$ | 200 V | $1\times10^{16}$ cm$^{-2}$ | Pulsed | 350°C | 10 min | 1 |
| TOPCon | Half | $H_2$ | 2500 V | $5\times10^{15}$ cm$^{-2}$ | Pulsed | 350°C | 10 min | 1 |
| TOPCon | Half | $H_2$ | 4800 V | $5\times10^{14}$ cm$^{-2}$ | Pulsed | 350°C | 10 min | 1 |
| TOPCon | Half | $H_2$ | 4800 V | $1\times10^{16}$ cm$^{-2}$ | Pulsed | 350°C | 10 min | 1 |
| TOPCon | Half | $H_2$ | 200 V | $1\times10^{16}$ cm$^{-2}$ | Continuous | 350°C | 10 min | 2 |
| TOPCon | Half | $H_2$ | 4800 V | $5\times10^{14}$ cm$^{-2}$ | Continuous | 350°C | 10 min | 2 |
| TOPCon | Half | $H_2$ | 4800 V | $5\times10^{14}$ cm$^{-2}$ | Pulsed | 350°C | 10 min | 2 |

In this last campaign of measurement, implantation on half TOPCon solar cells was this time investigated varying the type of gas ($H_2$ and $O_2$), the plasma mode, the potential and the dose. Similar to previous campaigns, several cells have been kept un-implanted to observe and quantify the evolution of the pseudo-performances after annealing. This annealing process has been performed at a temperature of 350°C for 10 minutes. To give a statistical overview of the $H_2$ and $O_2$ every sub-conditions of implantation has been regrouped in Fig. 5.

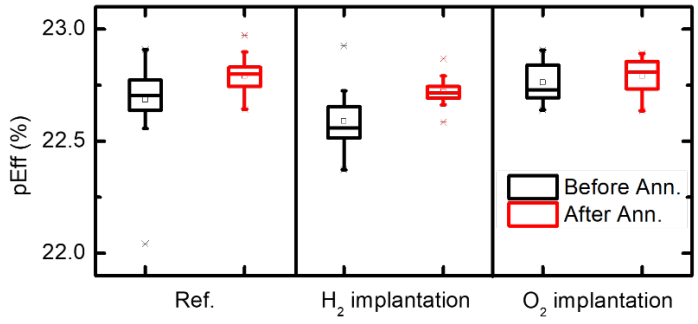


**FIGURE 5.** Pseudo-efficiency measured on TOPCon solar cells before and after annealing without prior implantation, before and after annealing with prior $H_2$ implantation and before and after annealing with prior $O_2$ implantation.

Hydrogen implanted half TOPCon cells show the same overall behavior than the SHJ half cells in the previous campaign. First a degradation of the pseudo-efficiency after the implantation, that is then recovered after annealing. However, Oxygen implanted cells show no degradation of the performances, even a slight increase can be observed after the implantation. But no more gain is obtained from the annealing treatment so that, the oxygen implanted and annealed cells are as efficient as the un-implanted but annealed cells. Figure 6 shows the pseudo-efficiency gains for the different investigated oxygen implantations compared with the un-implanted cells. In this figure, interesting results show a significative gain in the pseudo-efficiency just after the $O_2$ implantation in some of the low potential conditions. Such results are promising and need to be confirmed statistically.

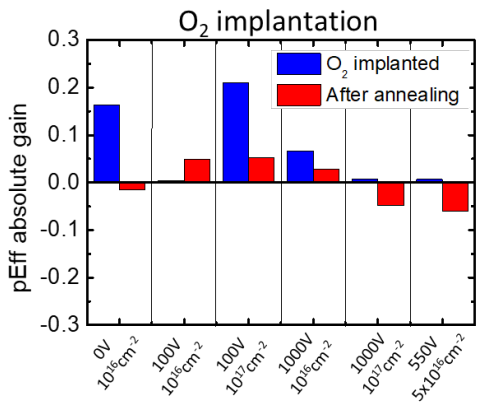


**FIGURE 6.** Absolute difference between the average pseudo-efficiency of each $O_2$ implanted cells and the average pseudo-efficiency of the un-implanted cells before and after annealing.

## CONCLUSION

The use of P-III using $H_2$ and $O_2$ plasma to passivate the cut edge of half SHJ and half TOPCon solar cells has been investigated showing no significant gain. In fact, the $H_2$ implantation degrades the performances of the cells. We have shown that not only the cut edges are damaged by such implantation but also the uncut edges can be impacted showing that in further studies those uncut edges need to be protected as well as the surfaces of the cells. If crystallographic defects left by the implanted hydrogen as it passes through the material are electrically actives, then DLTS measurements could help to characterize those defects and their density. The recovery of the performances after annealing could be explained by two different mechanisms: (i) Either the deposited hydrogen migrates toward the crystallographic defects to passivate them (ii) either the hydrogen is removed from the material. $H_2$ concentration could be measured before and after annealing to understand which mechanism is involved. Also, significant gains just after $O_2$ implantation have been observed on few TOPCon half cells. In consequences, P-III using $O_2$ to passivate the cut edge deserves to be thoroughly investigated.

## ACKNOWLEDGMENTS

This study has been founded by the BPI, REGION SUD and METROPOLE Aix-Marseille within the frame of the French project PASS-ION.

## REFERENCES

1. M.A. Green, E.D. Dunlop, J. Hohl-Ebinger, M. Yoshita, N. Kopidakis, and X. Hao, Progr. In Photovoltaics **29**, 657–667 (2021).
2. K. Yoshikawa, H. Kawasaki, W. Yoshida, T. Irie, K. Konishi, K. Nakano, T. Uto, et al., Nature Energy **2**, 1–8 (2017).
3. I. Haedrich, U. Eitner, M. Wiese, and H. Wirth, Solar Energy Materials And Solar Cells **131**, 14–23 (2014).
4. T. hee Jung, H. eun Song, H. keun Ahn, and G. hwan Kang, Solar Energy **103**, 253–262 (2014).
5. S. Guo, J.P. Singh, I.M. Peters, A.G. Aberle, and T.M. Walsh, International Journal Of Photoenergy **2013**, 1–8 (2013).
6. J. Müller, D. Hinken, S. Blankemeyer, H. Kohlenberg, U. Sonntag, K. Bothe, T. Dullweber, et al., IEEE Journal Of Photovoltaics **5**, 189–194 (2014).
7. M. Mittag, T. Zech, M. Wiese, D. Blasi, M. Ebert, and H. Wirth, "Cell-to-Module (CTM) Analysis for Photovoltaic Modules with Shingled Solar Cells" Proceedings of the IEEE 44th Photovoltaic Specialist Conference (PVSC), 2017, pp. 1531–1536.
8. A. Joshi, A. Khan, and A. Sp, "Comparison of half cut solar cells with standard solar cells" Proceedings of the Advances In Science And Engineering Technology International Conferences, 2019, pp. 1–3.

9. J. Shahid, A.Ö. Karabacak, and M. Mittag, "Cell-To-Module (CTM) Analysis for Photovoltaic Modules with Cell Overlap", Proceedings of the 30th PV Solar Energy Conference, 2020.
10. M. Mittag, A. Pfeundt, and J. Shahid, "Impact of Solar Cell Dimensions on Module Power, Efficiency and Cell-To-Module Losses", Proceedings of the 30th PV Solar Energy Conference (PVSEC-30), 2020, pp. 1–6.
11. L. Tous, J. Govaerts, S. Harrison, C. Carriere, F. Buchholz, A. Halm, A. Faes, et al., " Overview of the Latest Results Achieved in the H2020 Funded Project Highlight Aiming for HIGH-Performance, Low-Cost and Sustainable c-Si Modules Tailored for Different Applications", Proceedings of the 37th European Photovoltaic Solar Energy Conference and Exhibition, 2021.
12. H. Stolzenburg, A. Fell, F. Schindler, W. Kwapil, A. Richter, P. Baliozian, and M.C. Schubert, "Edge recombination analysis of silicon solar cells using photoluminescence measurements" Proceedings of the AIP Conference Proceedings, 2019, pp. 1–6.
13. J. Lelièvre, S. Harrison, M. Albaric, L. Carton, B. Portaluppi, and V. Barth, "Laser Cut 45 ° Rotated Ingot" Proceedings of the37th European Photovoltaic Solar Energy Conference And Exhibition, 2020,pp. 487–489.
14. D.D. Tune, F. Buchholz, I. Ullman, and A. Halm, "Measuring and Mitigating Edge recombination in Modules Employing Cut Cells", Proceedings of the 37th European Photovoltaic Solar Energy Conference And Exhibition, 2020, pp. 1689–1699.
15. B. Portaluppi, S. Harrison, and C. Carrere, "Development and Optimization of Shingle Heterojunction Modules" In Journée Nationales du Photovoltaïque, 2020.
16. D.D. Tune, F. Buchholz, I. Ullman, and A. Halm, "Measuring and Mitigating Edge recombination in Modules Employing Cut Cells", Proceedings of the 37th European Photovoltaic Solar Energy Conference And Exhibition, 2020, pp. 1689–1699.
17. S. Eiternick, K. Kaufmann, J. Schneider, and M. Turek, "Loss analysis for laser separated solar cells" Proceedings of the 4th International Conference On Silicon Photovoltaics, SiliconPV, 2014, pp. 326–330.
18. A. Münzer, P. Baliozian, K. Ahmed, A. Nair, E. Lohmüller, T. Fellmeth, A. Spribille, et al., "Laser Assisted Separation Processes for Bifacial pSPEER Shingle Solar Cells" Proceedings of the 37th European Photovoltaic Solar Energy Conference And Exhibition, 2020, pp. 1–9.
19. M. Bokalic, M. Kikelj, K. Brecl, M. Jankovec, F. Buchholz, V. Mihailetchi, and M. Topic, "El and Lbic Characterization of Cut Edge Recombination in Ibc" Proceedings of the 37th European Photovoltaic Solar Energy Conference And Exhibition, 2020, pp. 308–311.
20. F. Gérenton, J. Eymard, S. Harrison, R. Clerc, and D. Muñoz, Solar Energy Materials And Solar Cells **204**, 1–9 (2020).
21. P. Baliozian, E. Lohmüller, T. Fellmeth, N. Wöhrle, A. Krieg, and R. Preu, "Bifacial shingle solar cells on p-type Cz-Si (pSPEER)", AIP Conference Proceedings 1999, 1–6 (2018).
22. P. Baliozian, A. Munzer, E. Lohmuller, A. Nair, T. Fellmeth, N. Wohrle, H. Hoffler, *et al.*, IEEE Journal Of Photovoltaics **11**, 259–267 (2021).
23. P. Baliozian, A. Spribille, R. Preu, M. Al-Akash, E. Lohmuller, A. Richter, T. Fellmeth, *et al.*, IEEE Journal Of Photovoltaics **10**, 390–397 (2020).
24. B. Portaluppi, S. Harrison, V. Giglia, A. Sekkat, and D. Muñoz-rojas, "Insights on cell edge defects impact and post-process repassivation for heterojunction", Proceedings of the 37th European Photovoltaic Solar Energy Conference And Exhibition 2020, pp. 504–507.
25. V. Giglia, J. Veirman, R. Varache, B. Portaluppi, S. Harrison, and E. Fourmon, "Influence of edge recombinations on the performance of half-, shingled- and full silicon heterojunction solar cells" Proceedings of the37th European Photovoltaic Solar Energy Conference And Exhibition, 2020, pp. 282–285
26. T. Desrues, C. Oliveau, C. Seron, G. Borvon, F. Torregrosa, Q. Rafhay, A. Kaminski, et al., "Doping and Hydrogenation Processes for Passivating Contact Solar Cells Using Plasma Immersion Ion Implantation (PIII)" Proceedings of the EUPVSEC, 2020.
27. https://www.pv-magazine.com/2021/10/26/longi-achieves-25-82-efficiency-for-heterojunction-solar-cell/